Supporting Information

Influence of the Radicaloid Character of Polyaromatic Hydrocarbon Couplers on Magnetic Exchange Coupling

Prabhleen Kaur and Md. Ehesan Ali*

Institute of Nano Science and Technology, Sector-81, Mohali, Punjab 140306, India

E-mail: ehesan.ali@inst.ac.in

Ground state of coupler using Ovchinnikov's rule.
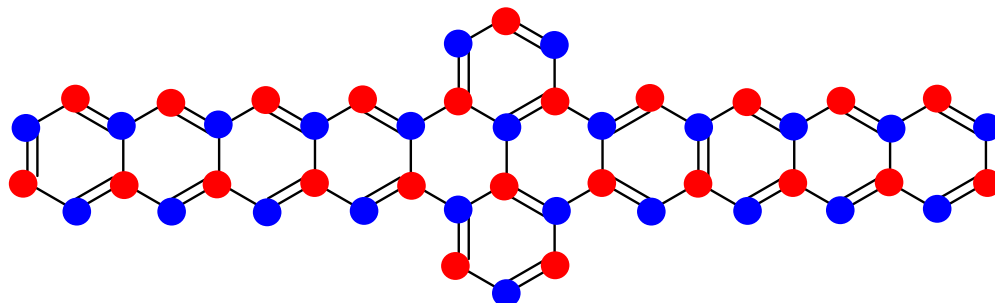
Figure S1: Two different types of carbon atoms in coupler b′ to illustrate Ovchinnikov's rule.

According to Ovchinnikov's rule, it is possible to predict the ground state multiplicity of the PAHs. There are two types of carbon atoms, such that each atom of a given color is chemically connected to only atoms with a different color (as illustrated in Figure R1 for coupler b′). The ground-state spin multiplicity (SM) of an alternant hydrocarbon is given by the difference between the number of sites of two colors,

$$SM = |n_{red} - n_{blue}| + 1$$

For the couplers used in this study, $n_{red} = n_{blue}$ thus giving SM=1 i.e. singlet spin-state. Ochinnikov's rule however cannot predict if the singlet state would have the closed-shell or open-shell nature.

Clar's Sextets in Couplers

Clar's theory has also been used to find the ground state properties of the PAHs. The maximum number of possible Clar's sextets in the coupler are shown in Figure R2. The recipe developed by Trinquier et al. (*J. Phys. Chem. A*, **2018**, 122, 1088-1103) has studied in detail the central rhombus part that predicts open-shell singlet as the ground state for diradical e′, but does not work for polyacene cases (coupler a′). Applying that recipe,
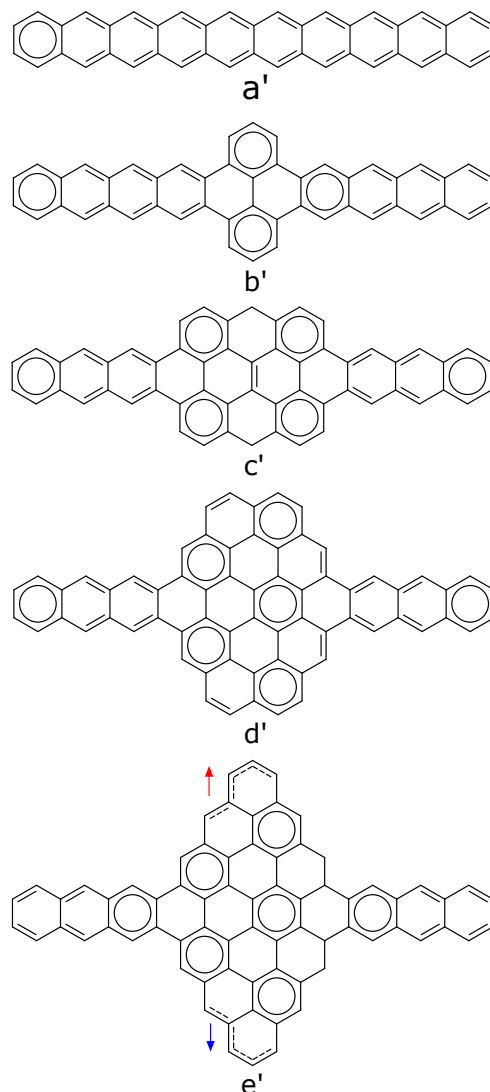
Figure S2: Clar sextets in all the couplers.

couplers b′, c′ and d′ have a closed shell singlet ground state.

Relative energies of different spin-states for diradicals a-e

Energies of different spin state with respect to triplet (ground state of all diradicals) for all diradicals **a-e** are plotted in Figure S2. The ground state of organic diradicals with couplers having substantial radicaloid character is predominantly determined by the spin
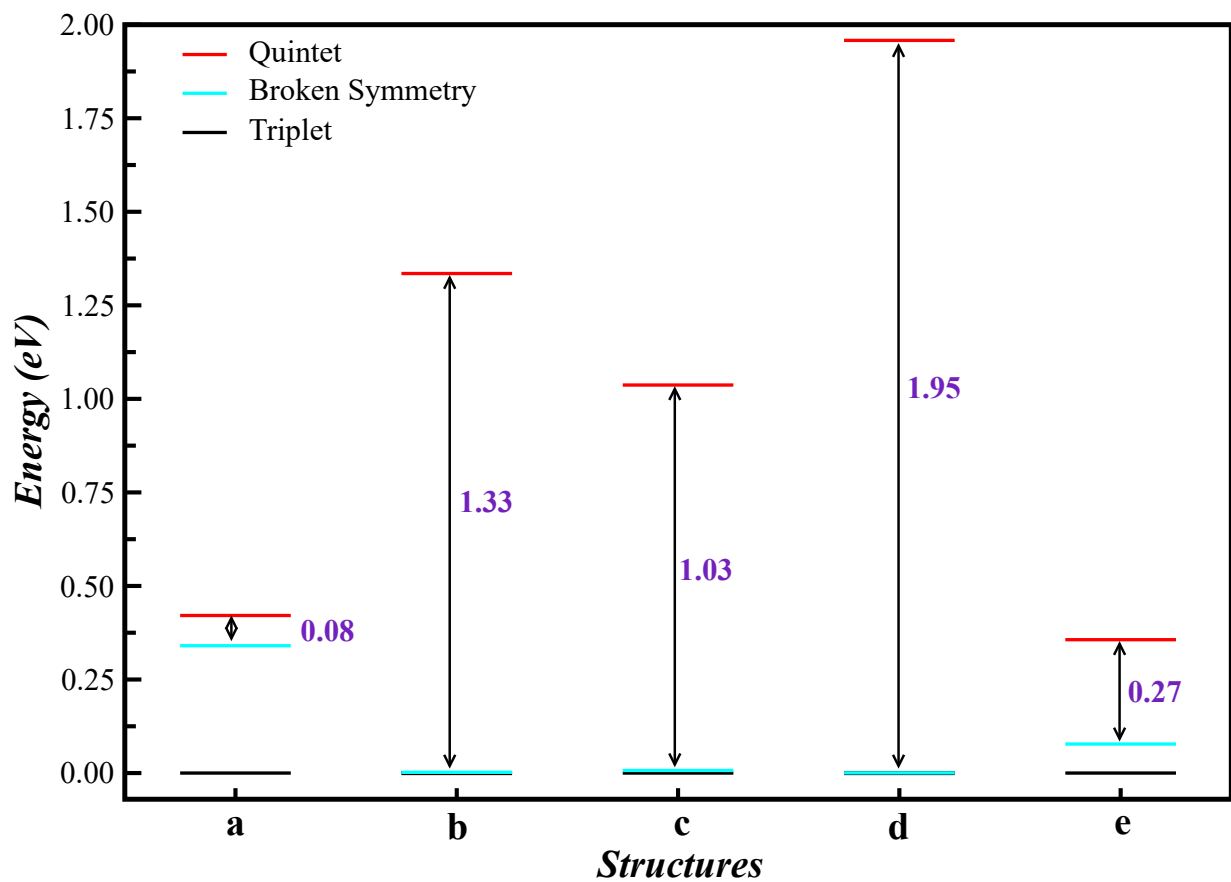
Figure S3: Relative energies of different spin states for all the structures evaluated using B3LYP/def2-TZVP method.

orientations at the nitroxy radical sites. The spins in the coupler owing to it's radicaloid property influence the molecular system in terms of higher spin state. More is the radicaloid character of the coupler, more closer is the quintet state to both triplet as well as BS state.

Para-connected diradicals

The evaluation of exchange coupling constants ($2J$) by connecting the nitroxide radicals at para positions was done by optimizing the diradicals in their BS state with B3LYP/def2-TZVP method and then computing $2J$ values at their BS optimized geometries. The radicaloid character was then calculated from the occupation number of natural orbitals of BS state obtained with UHF/def2-TZVP method. The results obtained are tabulated in Table S1.

Table S1: Computed magnetic exchange coupling ($2J$) (cm^{-1}) values and energies (Eh) with corresponding $<S^2>$ values of triplet (HS) and broken-symmetry (BS) states for all the diradicals ($\mathbf{a}_p$-$\mathbf{e}_p$) with B3LYP/def2-TZVP method. Radicaloid character of couplers when nitroxide radicals are attached to it (y_c), calculated using natural orbital occupancy of frontier orbitals obtained with UHF/def2-TZVP method.

Diradical	E_{HS} (Eh) $<S^2>_{HS}$	E_{BS} (Eh) $<S^2>_{BS}$	ΔE_{BS-T} (kcal/mol)	$2J$ (cm^{-1})	y_c
$\mathbf{a}_p$	-2107.722768 2.82	-2107.736915 2.32	-8.87	-6209.26	0.75
$\mathbf{b}_p$	-2337.570408 2.17	-2337.570479 1.19	-0.04	-30.96	0.31
$\mathbf{c}_p$	-2642.432561 2.11	-2642.432825 1.15	-0.16	-115.78	0.46
$\mathbf{d}_p$	-3024.688586 2.08	-3024.688603 1.08	-0.01	-7.48	0.17
$\mathbf{e}_p$	-3254.453818 2.08	-3254.453868 1.08	-0.03	-22.00	0.69

The radicaloid characters of the PAH spacers when nitroxy radicals are connected in pseudo-para positions are in accord with when radicals are connected in meta positions (Table 2).

The magnetic exchange coupling constants also vary with the respective radicaloid character of the connecting spacer with a maximum for diradical $\mathbf{a}_p$ and a minimum for $\mathbf{d}_p$. However, diradical $\mathbf{e}_p$ does not follow this rule. This can be understood from the spin-density plots of these para connected diradicals in their triplet and BS states (Figure S3). In spin-density plot for diradical $\mathbf{e}_p$ in its triplet state, no spin density is observed in the
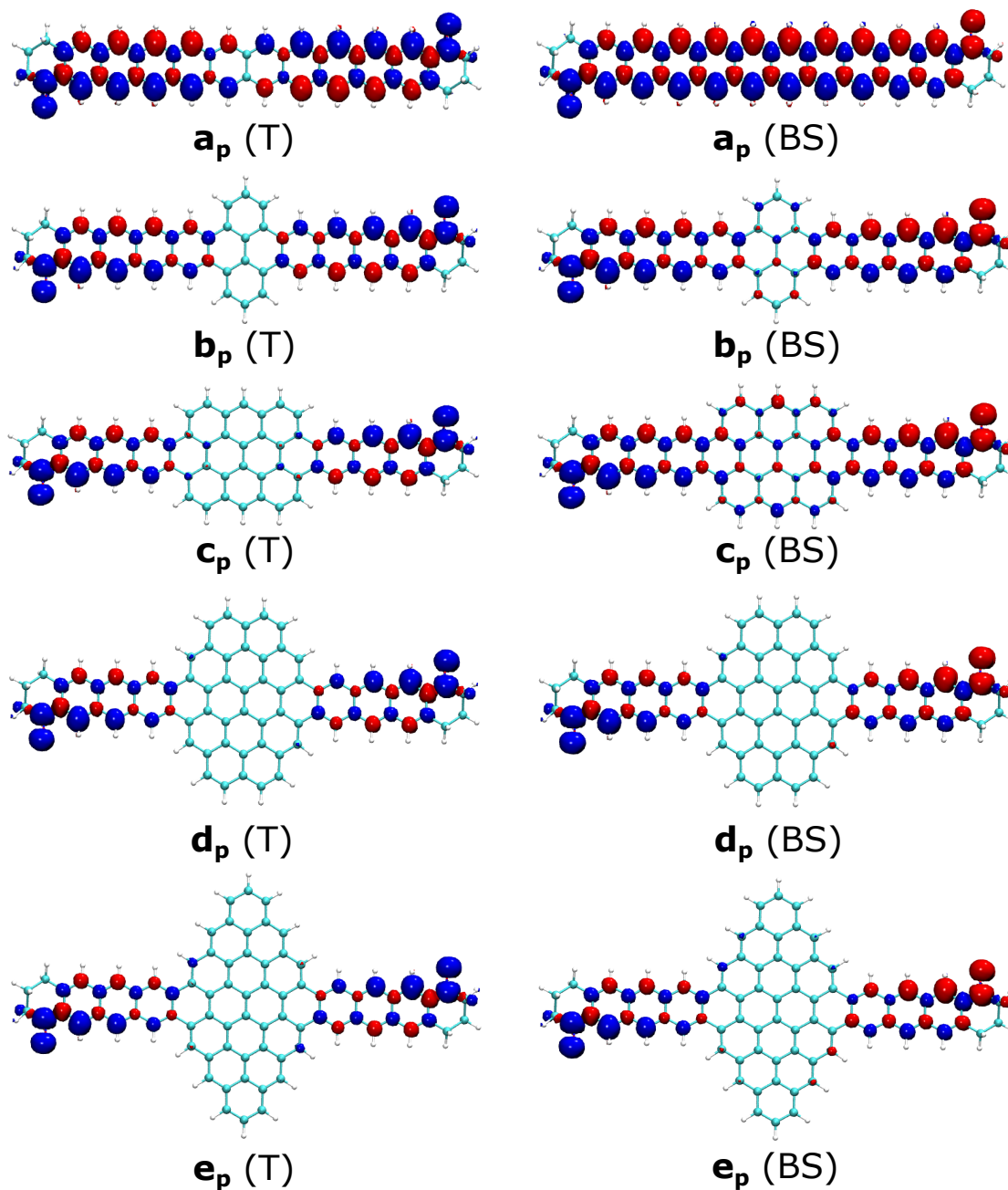
Figure S4: Spin-density plots of all the diradicals (**a-e**) in their triplet state (T) as well as broken-symmetry state (BS) with isosurface value $0.002\ e^-/\text{Å}^3$.

central region of the coupler as was observed in the meta connected diradical for the same coupler. This is also reflected in the $<S^2>$ value for the triplet state *2.08*, which indicates two spin system (nitroxy radicals) with no spin contamination despite the observed radicaloid character of the coupler. This may be due to the respective orientations

of the radical spins and the delocalized spin of the coupler. As can be seen from Figure 2, in triplet state with meta connected diradical **e** opposite spin moment delocalizes on the coupler in middle on the side connecting the same spin diradicals, which is not possible for para connected diradical. This also further indicates the importance of spin density profile in the coupler along with its radicaloid character.

Selected MOs of diradicals (a-e)

Diradical a
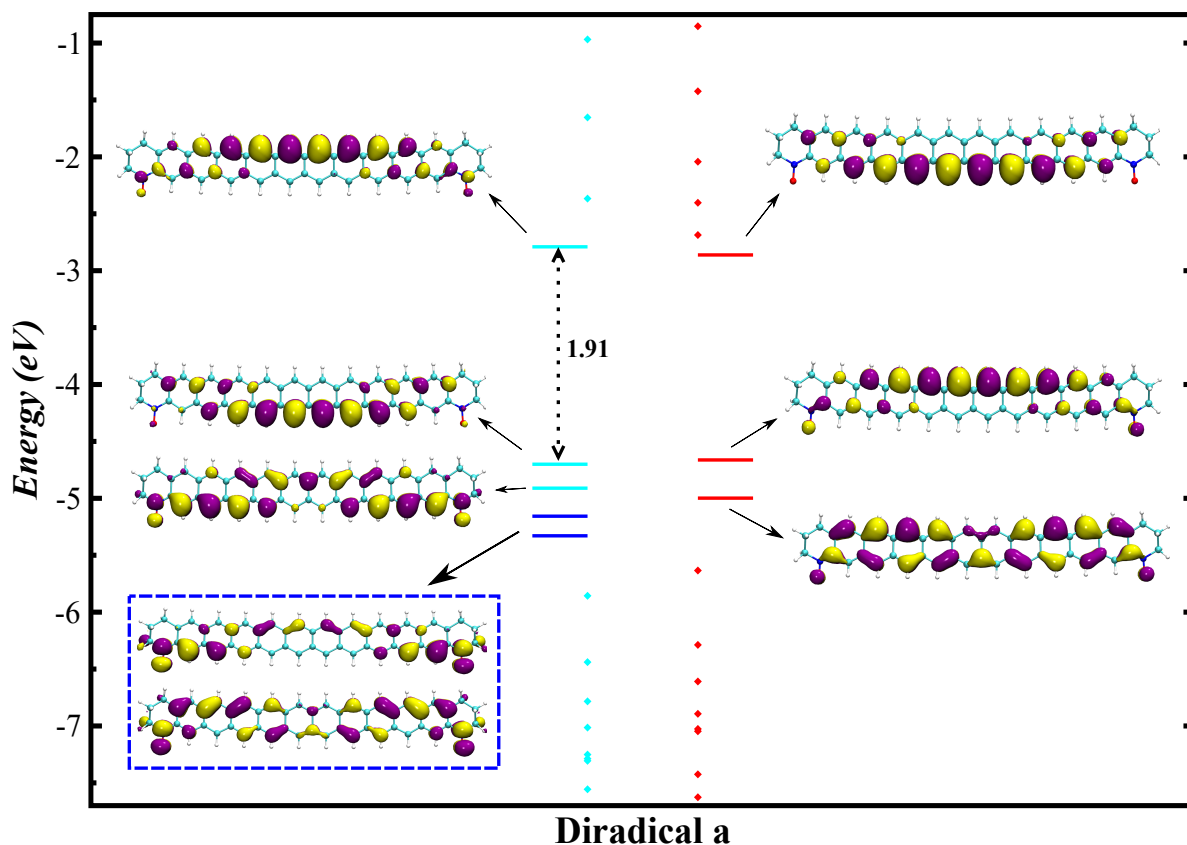
Figure S5: MOs of diradical **a** in it's triplet state.

The frontier orbitals of diradical **a** are from the coupler decacene. They are from dif-

ferent zigzag edge of decacene that are responsible for couplers' OSS nature. Due to interaction of nitroxy SOMOs with these open-shell orbitals of the coupler, they are stabilized in energy and are no longer the frontier orbitals. The degeneracy of nitroxy SOMOs is lifted up due to their asymmetric interactions with couplers' magnetic orbitals.

Diradical b
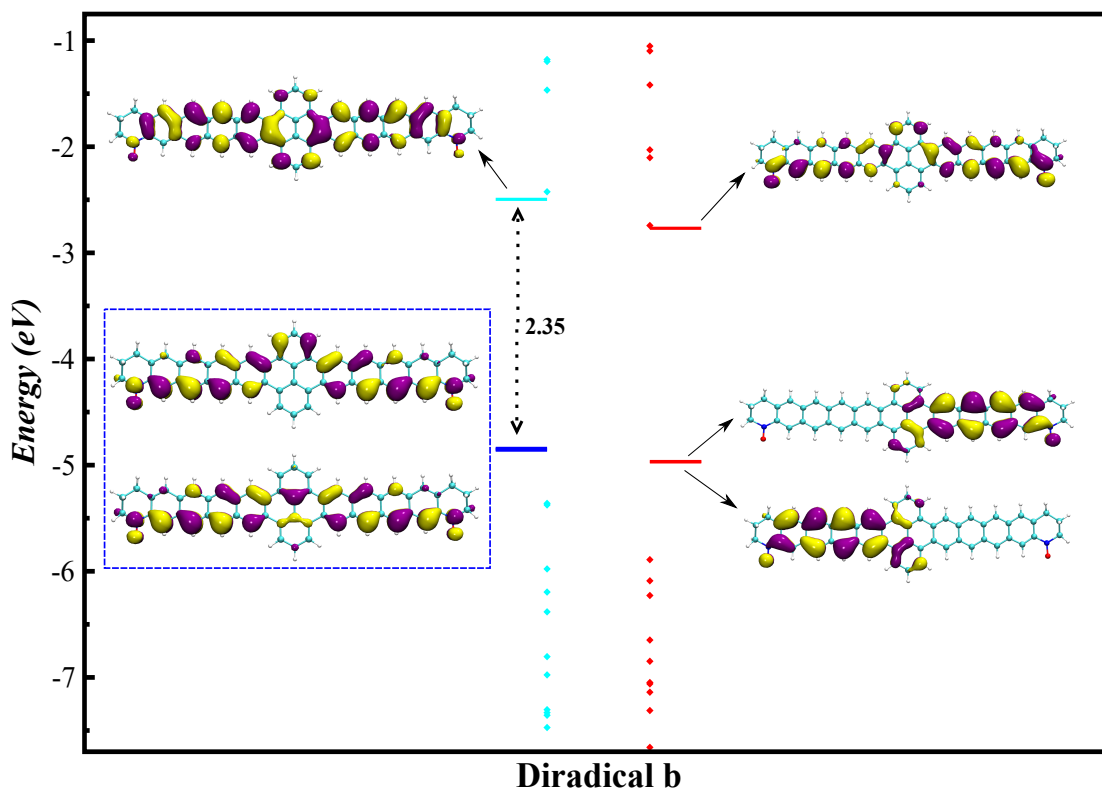
Figure S6: MOs of diradical **b** in it's triplet state.

The two additional benzenoid rings in the central region of decacene backbone reduces spin confinement and radicaloid character of coupler drastically. This results in nitroxy SOMOs be the frontier orbitals for diradical **b**.

Diradical c
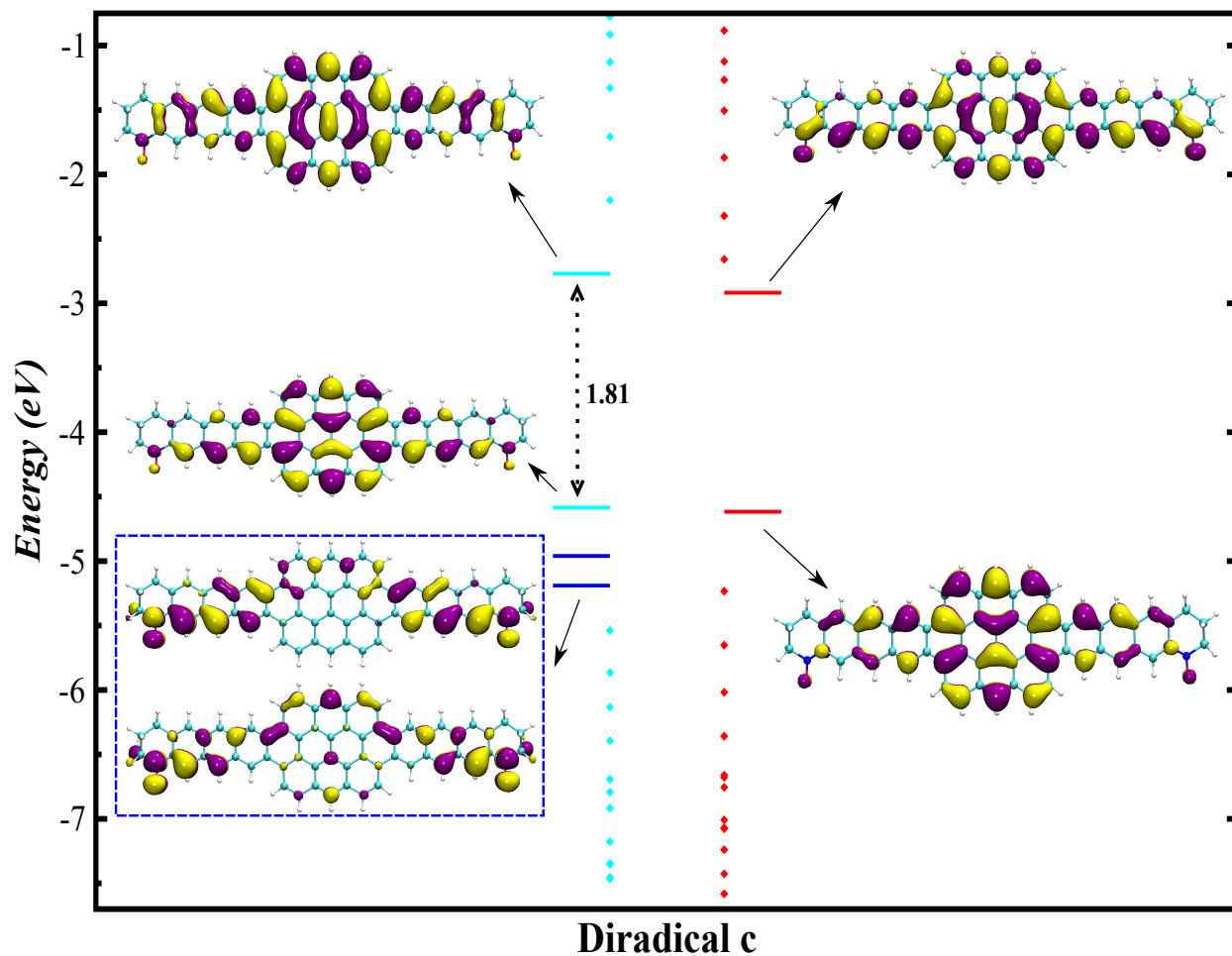
Figure S7: MOs of diradical **c** in it's triplet state.

Diradical **c** also have the frontier orbitals from the central region of the coupler, which are its magnetic orbitals. The orbital pictures of nitroxy SOMOs along with frontier orbitals indicate asymmetric interactions between them. Therefore, the degeneracy of the these SOMO's is lifted up.

Diradical d
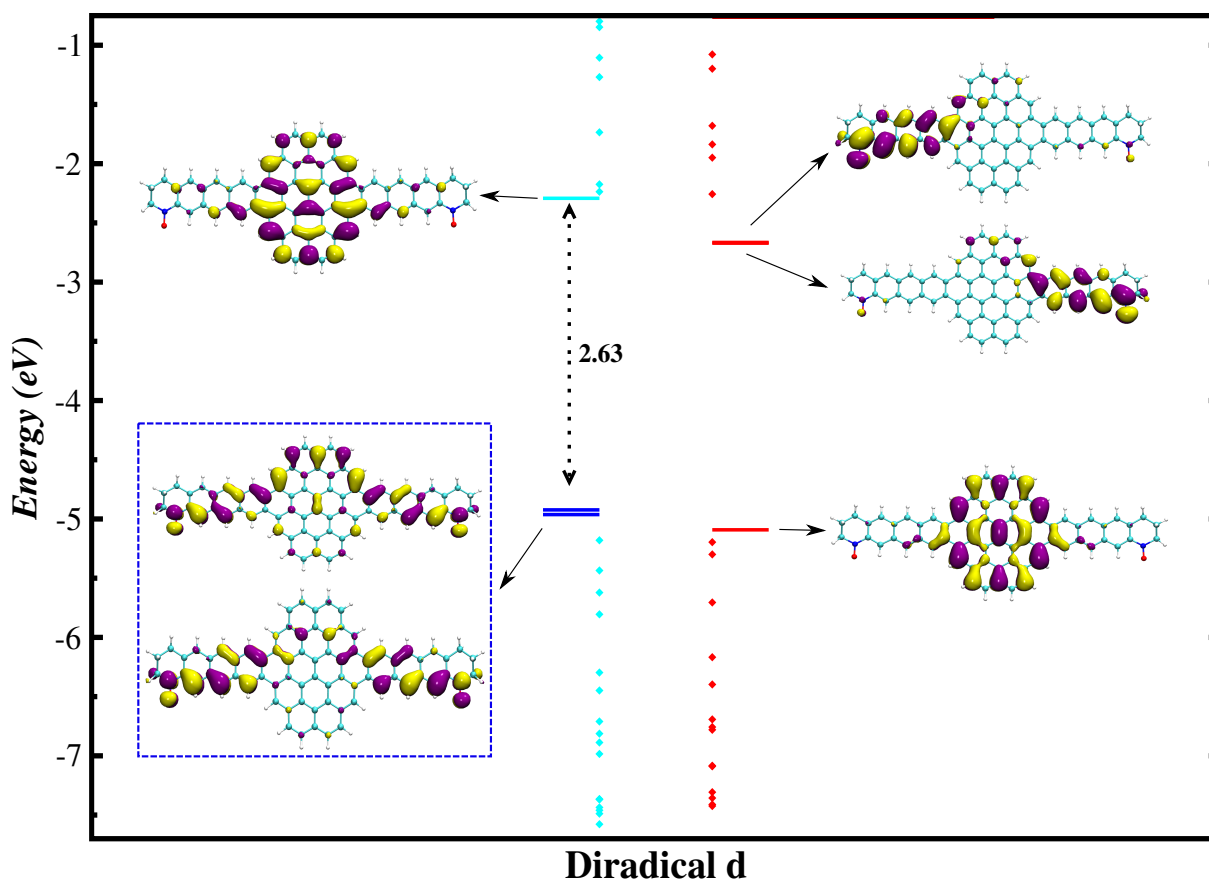
Figure S8: MOs of diradical **d** in it's triplet state.

Diradical **d** has the PAH coupler with the minimum radicaloid character. Therefore, MOs for this diradical depict degenerate nitroxy SOMOs as the frontier orbital.

Diradical e
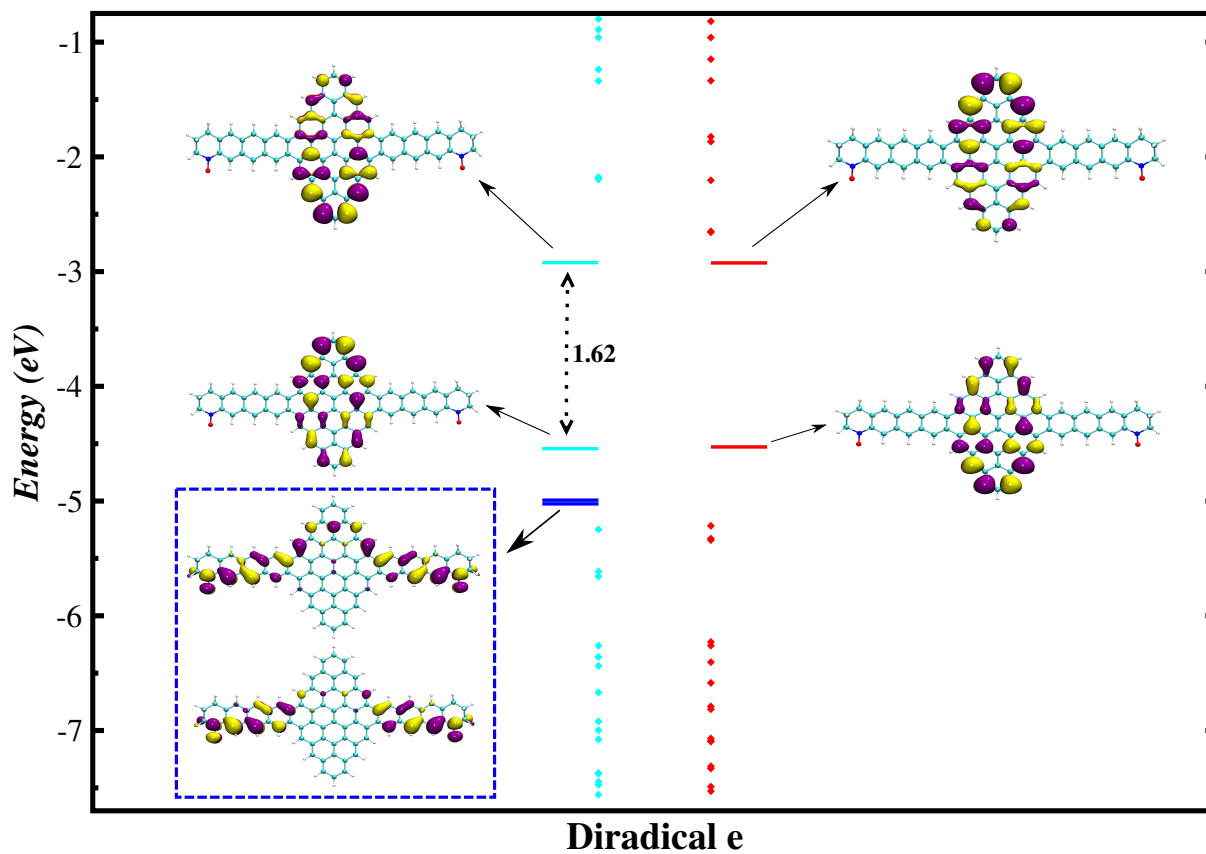
Figure S9: MOs of diradical **e** in it's triplet state.

Owing to large radicaloid character, magnetic orbitals of the coupler are also the frontier orbitals of diradical **e**. The nitroxy SOMOs and the couplers magnetic orbitals are well separated MOs spacially, therefore the interactions among them is symmetric. Hence, the nitroxy SOMOs in this diradical are degenerate in nature.

Comparison of diradical and coupler MOs
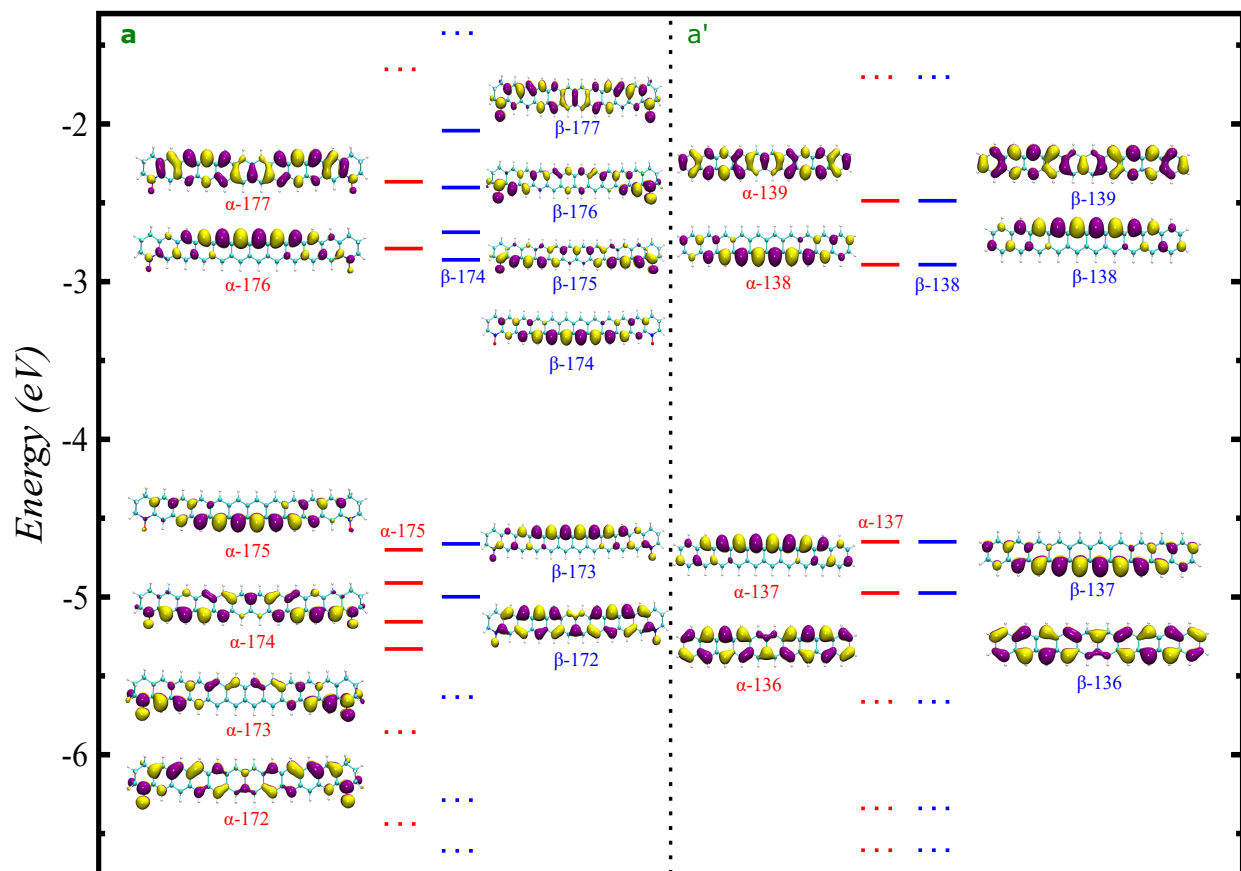
Figure S10: Energy level diagram for molecular orbitals of diradical **a** (left) and coupler a′ (right). α-orbitals are represented with red lines, while β-orbitals are shown with blue. The MOs shown with solid lines have pictorial representations as shown with the MO numbers as obtained in their respective single point calculation.
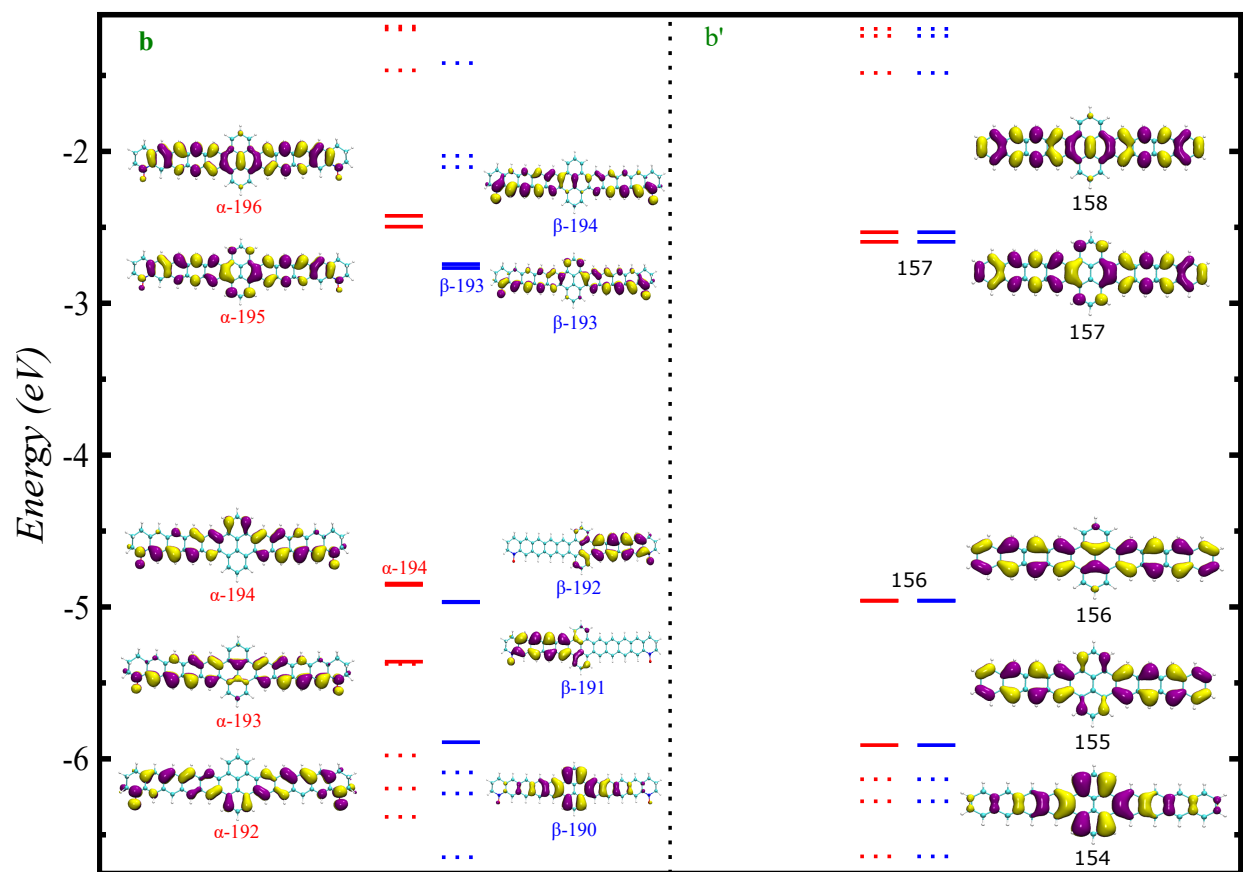
Figure S11: Energy level diagram for molecular orbitals of diradical **b** (left) and coupler b′ (right). α-orbitals are represented with red lines, while β-orbitals are shown with blue. The MOs shown with solid lines have pictorial representations as shown with the MO numbers as obtained in their respective single point calculation.
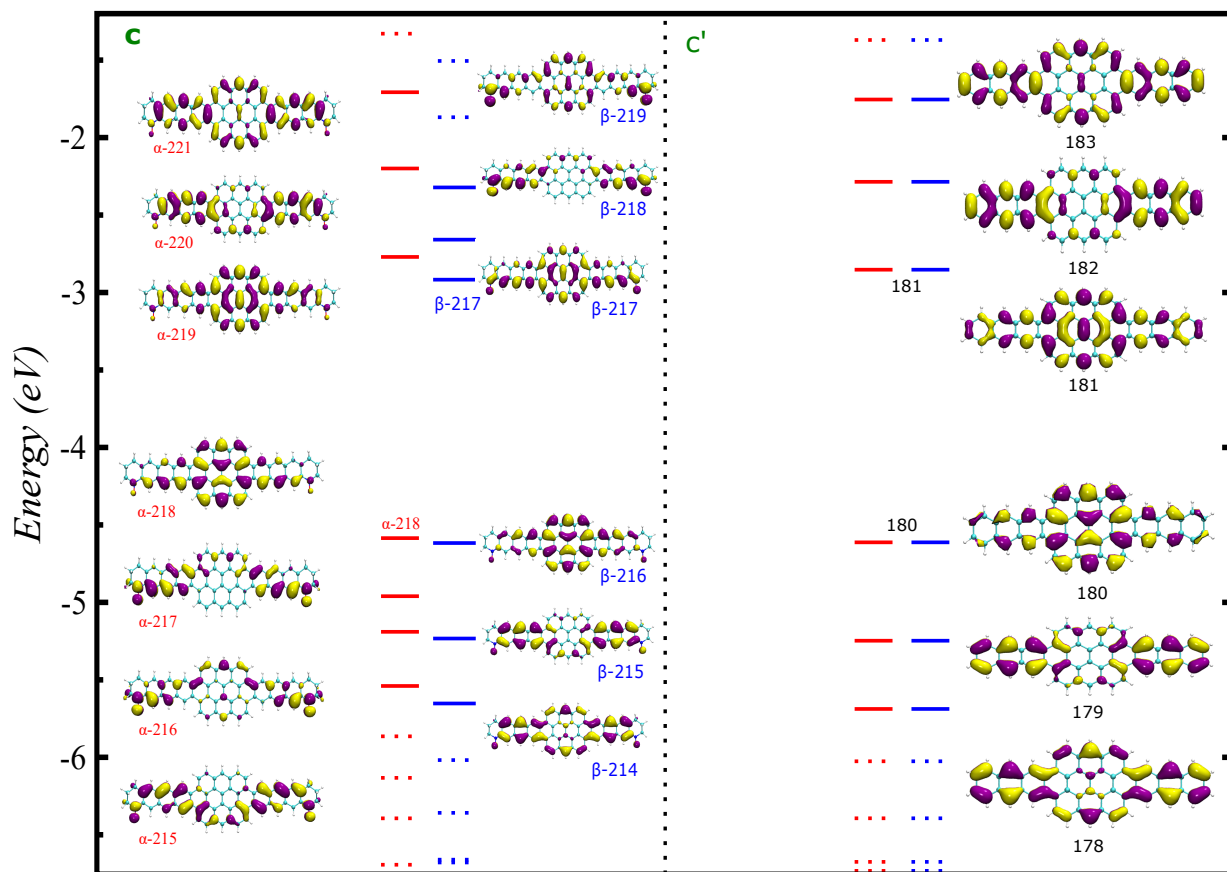
Figure S12: Energy level diagram for molecular orbitals of diradical **c** (left) and coupler c' (right). α-orbitals are represented with red lines, while β-orbitals are shown with blue. The MOs shown with solid lines have pictorial representations as shown with the MO numbers as obtained in their respective single point calculation.
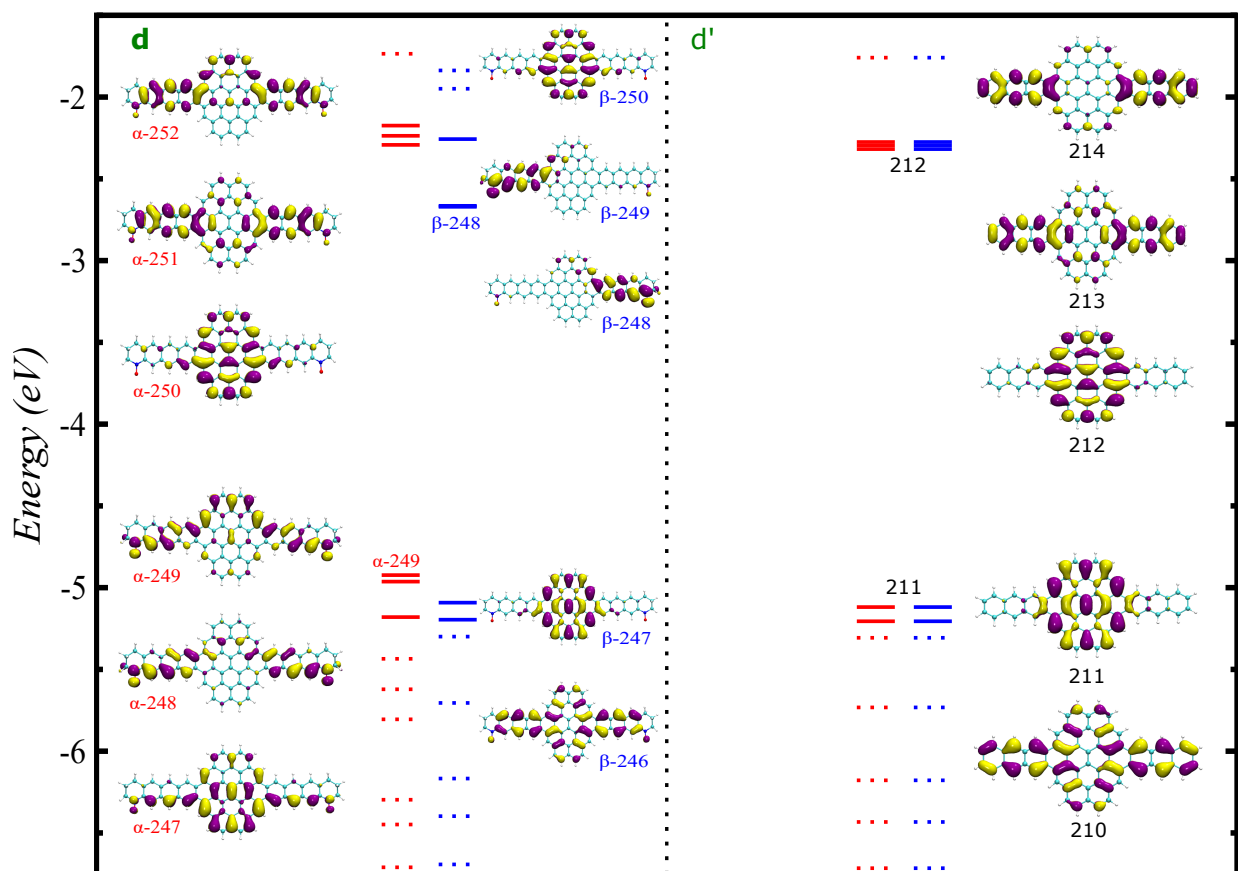
Figure S13: Energy level diagram for molecular orbitals of diradical **d** (left) and coupler d′ (right). α-orbitals are represented with red lines, while β-orbitals are shown with blue. The MOs shown with solid lines have pictorial representations as shown with the MO numbers as obtained in their respective single point calculation.
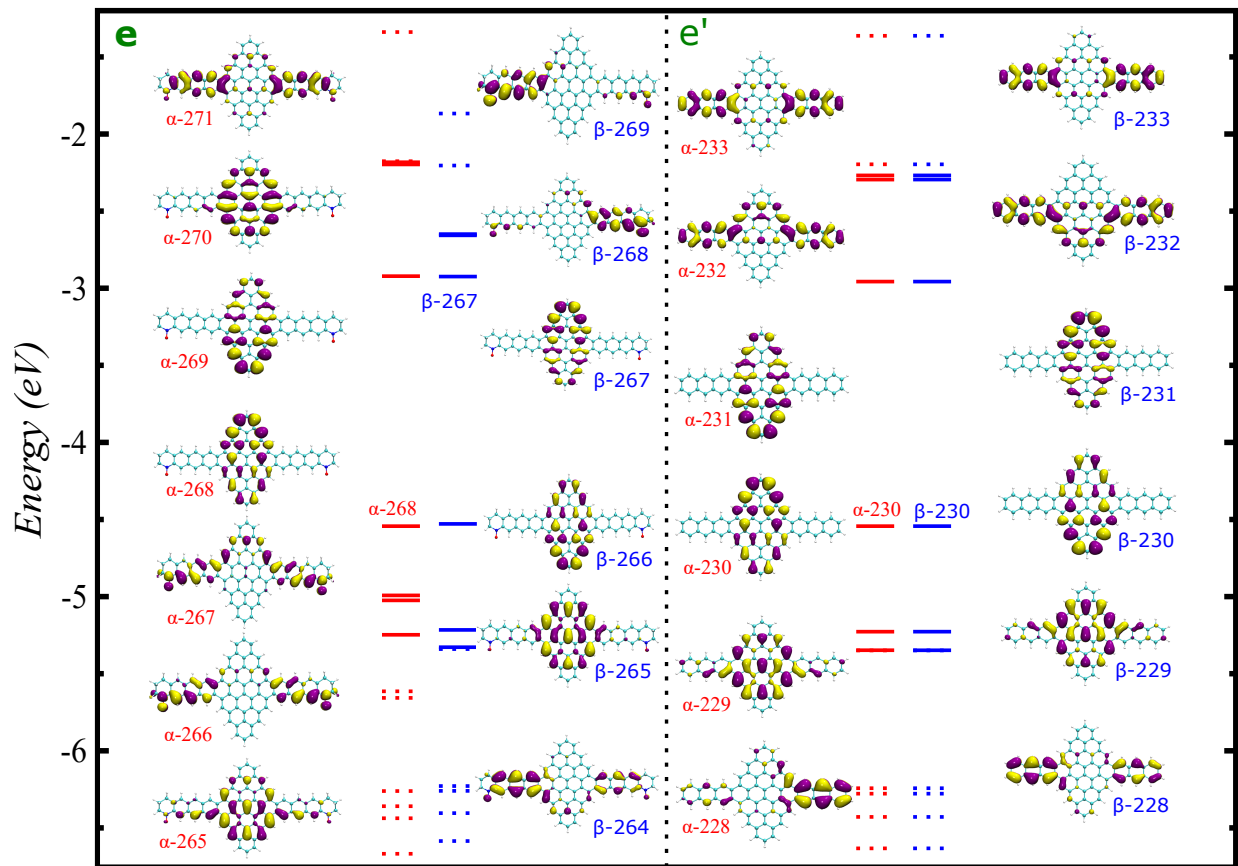
Figure S14: Energy level diagram for molecular orbitals of diradical **e** (left) and coupler e′ (right). *α*-orbitals are represented with red lines, while *β*-orbitals are shown with blue. The MOs shown with solid lines have pictorial representations as shown with the MO numbers as obtained in their respective single point calculation.

Applying Yamaguchi's triplet contamination from singlet state to obtain $E_S - E_T$ gap for PAH couplers

$$E_{Singlet}^{SP} = E_{Singlet} + [\chi(E_{Singlet} - E_{Triplet})] \tag{S1}$$

$$\chi = \frac{(^1\!\!<S^2> /^3\!<S^2>)}{1 - (^1\!\!<S^2> /^3\!<S^2>)} \tag{S2}$$

In order to remove triplet spin contamination from a singlet wavefunction, above equations (Eqs. S1 and S2) as proposed by Yamaguchi et al. (Yamaguchi et al. *Theor. Chim. Acta*, **1988**, 73, 337-364) can be used and hence singlet-triplet gap could be calculated. In the literature it is approximated $E_{BS} \sim E_S$ when the system is symmetric (Ruiz et al. *J. Comput. Chem.*, **2003**, 24, 983-989, Perdew et al. *Int. J. Quantum Chem.*, **1997**, 61, 197, Ruiz et al. *J. Am. Chem. Soc.*, **1997**, 119, 1297) which is employed in above formulaes for these systems. Therefore, $E_{BS}=E_S$ for b′, c′ and d′ as $^1\!<S^2>=0$ for these couplers. The resulting $E_S - E_T$ gap using the decontamination formulas is tabulated in Table S2:

Table S2: $E_S - E_T$ gap calculated using removal of triplet decontamination from singlet wavefunction as formulated by Yamaguchi and co-workers (Eqs. S1 and S2).

PAH coupler	χ	ΔE_{S-T} (kcal/mol)	y_p
a′	2.12	-16.23	0.92
b′	0	-27.98	0.34
c′	0	-21.92	0.50
d′	0	-45.14	0.25
e′	0.44	-10.51	0.74

Applying the formulas, we obtain least $E_S - E_T$ gap for e′ and not for a′. These results do not reflect the required inverse relation between ΔE_{S-T} and y (Hayashi et al. *J. Am. Chem. Soc.*, **2020**, 142, 20444-20455). Therefore, this method can not be used for systems with intrinsic moderate to high radicaloid character to obtain $E_S - E_T$ gap.